Magnetic ordering in $HoBaCo_2O_{5.5}$

J.-E. Jørgensen[1,*] and L. Keller[2]
[1]*Department of Chemistry, University of Aarhus, DK-8000 Århus C, Denmark*
[2]*Laboratory for Neutron Scattering, ETH Zurich and Paul Scherrer Institut, CH-5232 Villigen PSI, Switzerland*
(Received 14 May 2007; revised manuscript received 29 September 2007; published 28 January 2008)

The crystal and magnetic structures of $HoBaCo_2O_{5.5}$ have been studied by neutron powder diffraction in the temperature range from 20 to 330 K. The crystal structure of $HoBaCo_2O_{5.5}$ was found to be best described in space group *Pmma* on a $2a_p \times 2a_p \times 2a_p$ unit cell where a_p refers to the lattice parameter of the cubic perovskite unit cell. The *a* and *b* axes were found to decrease and increase abruptly within the temperature range from 290 to 315 K as the temperature increases, and the unit-cell volume exhibits an excess thermal expansion in the temperature range from 230 to 290 K. The anomalous changes in lattice parameters and unit-cell volume were attributed to the metal-insulator transition and spin-state changes of the Co^{3+} ions. The magnetic structure of $HoBaCo_2O_{5.5}$ was shown to be antiferromagnetic with a $2a_p \times 2a_p \times 4a_p$ magnetic unit cell containing four crystallographically independent Co ions, two octahedrally coordinated and two pyramidally coordinated. The refined low temperature values of the magnetic moments of the Co ions indicated that one set of octahedrally coordinated Co^{3+} ions were in the high-spin state while the other set of octahedrally coordinated Co^{3+} ions were in mixed intermediate- and low-spin states. The pyramidally coordinated Co^{3+} ions were found to be in the intermediate-spin states.

DOI: 10.1103/PhysRevB.77.024427 PACS number(s): 75.25.+z

I. INTRODUCTION

Systems with strongly correlated electrons such as many transition-metal oxides show coupling between charge, orbital, and spin degrees of freedom. The rare-earth cobaltites $RBaCo_2O_{5+\delta}$ (R=Y or rare-earth element) are representatives of such systems, and they have been the subject of intense studies in recent years. The large allowed oxygen range ($0 \leqslant \delta \leqslant 1$) leads to several crystallographic structures, mixed-valence states of the cobalt ions (oxidation states 2+, 3+, and 4+) as well as a complex interplay between charge, spin-orbital, and lattice degrees of freedom. Magnetic ordering accompanied by colossal magnetoresistance as well as metal-insulator (MI) transitions have been observed in this family of compounds.[1–5] $RBaCo_2O_{5+\delta}$ compounds with $\delta < 1$ are oxygen-deficient perovskites, and the wide allowed oxygen range leads to several different crystallographic structures, with either square pyramidal or octahedral (or both) coordination of cobalt.[1,2,4] The basic $RBaCo_2O_5$ structure corresponds to a doubling of the primitive perovskite unit cell, and it is described as an $a_p \times a_p \times 2a_p$ structure, where $a_p \approx 3.9$ Å refers to the lattice parameter of the primitive cubic perovskite unit cell. $RBaCo_2O_{5+\delta}$ has for $\delta=0$ a layer structure in which oxygen is absent in the *R* layers and all cobalt atoms are pyramidally coordinated. In the case of $\delta=1$ all cobalt atoms are octahedrally coordinated and the layered structure is not as evident as for $\delta=0$. The layered structure only results from a complete ordering of the *R* and Ba atoms for compounds with $\delta=1$. Compounds with a large difference between *R* and Ba radii tend to be ordered and thereby layered. The exact crystal structure of compounds with $\delta \neq 0$ and 1 is in many cases still not clearly established, and especially for $\delta=0.5$ conflicting results have been obtained. The crystal structures the $RBaCo_2O_{5.5}$ compounds have been described on $a_p \times 2a_p \times 2a_p$, $2a_p \times 2a_p \times 2a_p$, and $2a_p \times 2a_p \times 4a_p$ unit cells with the Co^{3+} ions equally distributed in square pyramidal and octahedral coordination.[1,2,5]

The magnetic behavior of the $RBaCo_2O_{5+\delta}$ compounds is rather complex due to the fact that the Co ions can adapt different spin states. Furthermore, charge-ordering processes are possible for compounds with $0 \leqslant \delta < 0.5$ and $0.5 < \delta \leqslant 1$. Here we will be concerned with the magnetic structure of compounds with formula $RBaCo_2O_{5.5}$ which contains Co^{3+} ions only and therefore do not exhibit charge ordering. Co^{3+} is a $3d^6$ ion, and as a result of the competition between intra-atomic exchange and the effect of the crystal field, it can exist in the low-spin (LS) state ($t_{2g}^6 e_g^0$, $S=0$) and the intermediate-spin (IS) state ($t_{2g}^5 e_g^1$, $S=1$) as well as the high-spin (HS) state ($t_{2g}^4 e_g^2$, $S=2$).[6] The gaps between these states are rather small and in the range 30–100 meV,[7,8] and changes from the LS to the IS and HS states are therefore possible as the temperature increases. The temperature-induced spin-state changes may be accompanied by changes in the magnetic structure as well as spin-state-ordering transitions which have been studied by neutron diffraction and magnetization measurements.[9–12]

Several studies of the magnetic structure of the $RBaCo_2O_{5+\delta}$ compounds with $\delta \approx 0.5$ have been performed with diverging results. A neutron diffraction study of $NdBaCo_2O_{5.47}$ showed that the IS Co^{3+} spins order in a *G*-type antiferromagnetic structure at 275 K and a spin-state ordering was found to take place at 230 K. In the spin-state-ordered phase every second octahedral Co^{3+} ion along the *a* axis is in the diamagnetic LS state while the remaining Co^{3+} ions are in the IS state. The IS Co^{3+} ions also form columns along the *c* axis. It was found that the spin-state-ordered phase forms clusters with a correlation length of 350 Å and it coexists with the *G*-type antiferromagnetic phase.[10] However, an additional study of $NdBaCo_2O_{5.5}$ revealed no long-range magnetic ordering, but weak diffuse scattering was observed. The diffuse reflections were indexed on the following unit cells: a $2\sqrt{2}a_p \times 2\sqrt{2}a_p \times 2a_p$ cell for $300 \geqslant T$

$\geqslant 250$ K and $2\sqrt{2}a_p \times 2\sqrt{2}a_p \times 4a_p$ cell for $T \leqslant 200$ K, but the weakness of these reflections prevented further analysis.[5] Soda *et al.* have performed a neutron single-crystal diffraction study of $NdBaCo_2O_{5.5}$, and it was found that this compound orders antiferromagnetically with a noncollinear *G*-type structure.[13] Taskin *et al.* proposed a model for the magnetic structure of $GdBaCo_2O_{5.5}$ in which all octahedral Co^{3+} ions are in the LS state while the pyramidal Co^{3+} ions are in the IS state.[12] The pyramidal Co^{3+} ions order ferromagnetically along [1,0,0], and the coupling between the ferromagnetically ordered planes is antiferromagnetical along the [0,1,0] direction. The model was based upon a magnetization measurement of a detwinned single crystal. The structure of $TbBaCo_2O_{5+\delta}$ with $\delta \approx 0.5$ has been studied by several groups starting with the work by Moritomo *et al.*[14] No magnetic structure was determined at 50 K. Later, the magnetic structure of this compound was studied by Khalyavin *et al.*[9] Their work showed that fast-cooled $TbBaCo_2O_{5.4}$ orders antiferromagnetically in a canted *G*-type structure. It was furthermore demonstrated that the magnetic-ordering process depends on the degree of oxygen order and thereby on the cooling rate of the samples during synthesis. Fast-cooled samples were shown to develop a spontaneous magnetization and to exhibit a ferromagnetic to antiferromagnetic transition. Recently, a detailed study of the spin-structure magnetic phase transitions in $TbBaCo_2O_{5.5}$ was performed by Plakhty *et al.*[15] It was found that $TbBaCo_2O_{5.5}$ orders ferrimagnetically at $T \approx 290$ K and this magnetic phase transforms to an antiferromagnetic phase as $T \approx 255$ K. A second antiferromagnetic phase was observed below 170 K. In the present work, we present a neutron powder diffraction study of the crystal structure of and the magnetic ordering in $HoBaCo_2O_{5.5}$.

II. EXPERIMENTAL DETAILS

The $HoBaCo_2O_{5.5}$ sample was prepared by solid-state synthesis by mixing stoichiometric amounts of Ho_2O_3, $BaCO_3$, and Co_3O_4. The mixture was heated to 1000 °C for 12 h in air several times with intermediate grinding steps and finally to 1070 °C in O_2 flow for 12 h. The neutron diffraction data were collected on the DMC diffractometer at the Swiss spallation neutron source SINQ using a wavelength of 2.5657 Å. The sample was loaded into a helium-filled vanadium can mounted on a closed-cycle helium refrigerator, and powder patterns were collected in the temperature range from 20 to 330 K in the sequence 130, 230, 260, 290, 315, 330, 275, 240, and 20 K. Data analysis was performed by the Rietveld method using the FULLPROOF program package,[16] with the use of its internal tables for neutron-scattering lengths and magnetic form factors. The linear absorption coefficient was determined by a transmission measurement and used in refinements.

III. RESULTS AND DISCUSSION

Inspection of the measured powder patterns showed that magnetic ordering was present in patterns recorded for $T \leqslant 265$ K. Several trail refinements of structural models with different space groups were made to clarify the crystal structure of $HoBaCo_2O_{5.5}$ above this temperature. The following models with cells and space groups were tried: $a_p \times a_p \times 2a_p$ *Pmmm*, $a_p \times 2a_p \times 2a_p$ *Pmmm*, $2a_p \times 2a_p \times 2a_p$ *Pmma*, and $2a_p \times 2a_p \times 4a_p$ *Pcca*. It was found that the $2a_p \times 2a_p \times 2a_p$ *Pmma* and $2a_p \times 2a_p \times 4a_p$ *Pcca* models gave the best description of the powder patterns measured above 265 K, and the quality of the fits was almost identical for the two models. However, the very weak reflections allowed in the *Pcca* model were not observed in the experimental data and no indication of a doubling of the *c* axis was found. *Pcca* is a subgroup of *Pmma* and the *Pcca* model contains 24 structural parameters while the *Pmma* model contains just 17 structural parameters. The present data sets were measured with a relatively long neutron wavelength and therefore cover a fairly small $\mathbf{q}$ range ($\mathbf{q}_{max} = 3.74$ Å^{-1}). It was therefore not possible through Rietveld refinement to perform a reliable determination of the minor atomic displacements which distinguishes the two space groups. The final refinements of the crystal structure of $HoBaCo_2O_{5.5}$ were therefore made with the $2a_p \times 2a_p \times 2a_p$ *Pmma* model for $T > 265$ K as this model has the smallest number of structural parameters. The observed and calculated powder patterns at 330 K are shown in Fig. 1(a) and the structural parameters are given in Table I for $T > 265$ K. The crystal structure at 330 K is shown in Fig. 2 while the lattice parameters and the unit cell volume are plotted as a function of temperature in Fig. 3. The thermal expansion of $HoBaCo_2O_{5.5}$ is seen to be anisotropic as the *b* and *c* axes increase as a function of the temperature in the temperature range from 20 to 290 K while the *a* axis exhibits a tendency to negative thermal expansion. An abrupt change in the *a* and *b* axes takes place between 290 and 315 K as the *a* and *b* axes decrease and increase abruptly by −0.6 and +0.4%, respectively, and a minor increase of −0.1% is observed for the *c* axis. The temperature dependence of the unit-cell volume is also anomalous as an excess thermal expansion is observed in the temperature range from 230 to 290 K and a decrease of −0.04% takes place between 290 and 315 K.

Unfortunately, the relatively low accuracy of the refined oxygen positions makes it impossible to correlate the anomalous changes in the lattice parameters with changes in the coordination environment of the cobalt ions. The observed type of anomalous changes of the lattice parameters and unit-cell volumes has been observed in several $LnBaCo_2O_{5.5}$ compounds—e.g. for *L*=Gd and Tb—and it has been attributed to orbital ordering accompanied by a MI transition although a completely coherent picture has not yet emerged.[14,17,18] A high-resolution x-ray powder diffraction study of $GdBaCo_2O_{5.5}$ showed that the unit-cell volume expands linearly up the MI transition where an excess expansion of the volume was observed and the changes in the lattice parameters *a* and *b* were qualitatively the same as found in this study. The excess volume expansion was attributed to a change to higher-spin states of the Co^{3+} ions in the octahedral sites.[18] Recently, $HoBaCo_2O_{5.5}$ was studied by high-resolution neutron powder diffraction and differential scanning calorimetry (DSC) in the temperature range from 250 to 380 K. This study showed a drop of −0.15% of the unit-cell volume at the MI transition at 305 K accompanied

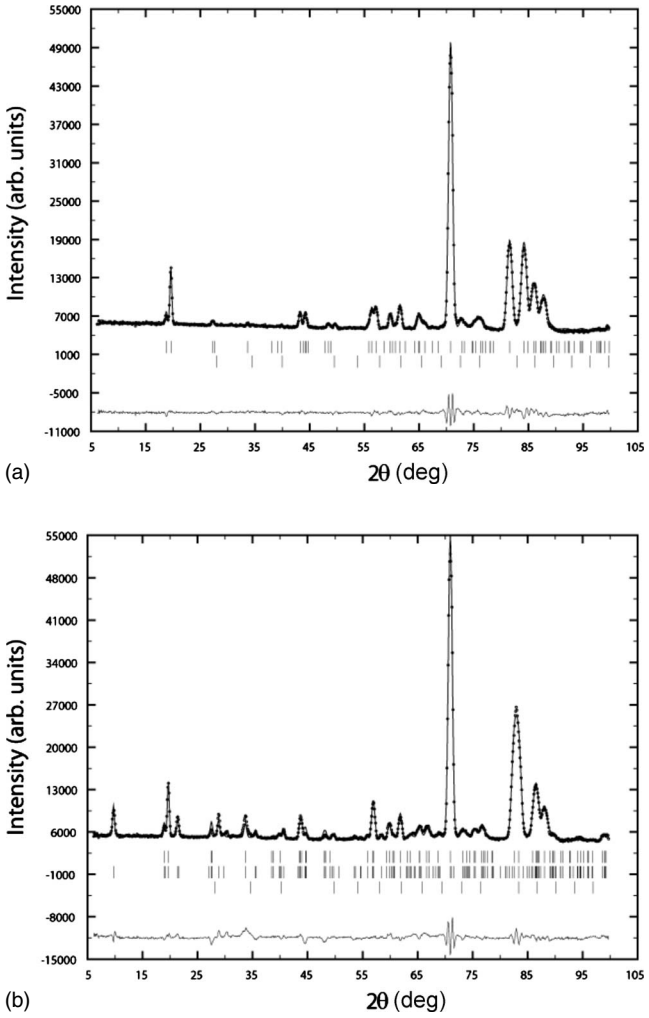

FIG. 1. Observed and calculated neutron powder diffraction profiles for $HoBaCo_2O_{5.5}$ at $T=330$ K (a) and 20 K (b). The difference between observed and calculated intensities is shown below the diffraction profiles in both plots. The positions of the Bragg peaks are marked with vertical bars. The upper and lower rows represent the $HoBaCo_2O_{5.5}$ and Ho_2O_3 impurity phases, respectively. The middle row of vertical bars in (b) represents the positions of the magnetic Bragg peak.

by melting of the orbital order in the pyramids. No change of symmetry was observed and the refinements of the crystal structures were performed in space group *Pmmm* at all temperatures. The DSC measurements indicated that the transition is of first-order type.[19] The onset of the excess volume expansion at 230 K, which is observed in this work, is rather remarkable as it starts within the magnetically ordered phase. It presumably originates from a change of spin state of the Co ions as the ionic radius increases with increasing spin multiplicity. The spin states of the four crystallographically different Co ions are discussed below. In the case of $GdBaCo_2O_{5.5}$ the excess volume expansion starts at 350 K and coincides with the MI transition while magnetic ordering takes place at 250 K in this compound.[18] The observed contraction of −0.1% of unit-cell volume is in agreement with what is usually observed in manganites and cobaltates during

TABLE I. Structural parameters for $HoBaCo_2O_{5.5}$. Space group *Pmma* (No. 51). Atomic positions: Ho 4*h* (0 *y* $\frac{1}{2}$) Ba 4*g* (0 *y* 0), Co(1) 2*e* (1/4 0 *z*), Co(2) 2*e* (1/4 0 *z*), Co(3) 2*f* (1/4 $\frac{1}{2}$ *z*), Co(4) 2*f* (1/4 1/2 *z*), O(1) 2*e* (1/4 0 *z*), O(2) 2*f* (1/4 1/2 *z*), O(3) 2*f* (1/4 1/2 *z*), O(4) 4*i* (*x* 0 *z*), O(5) 4*j* (*x* 1/2 *z*), O(6) 4*k* (1/4 *y* *z*), and O(7) 4*k* (1/4 *y* *z*). Lattice parameters *a*, *b*, and *c*. Weighted profile values R_{wp}.

T (K)		275	290	315	330
Ho	*y*	0.273(1)	0.2718(9)	0.270(1)	0.2670(1)
Ba	*y*	0.250(2)	0.251(2)	0.250(2)	0.252(2)
Co(1)	*z*	0.288(4)	0.268(4)	0.293(3)	0.290(2)
Co(2)	*z*	0.730(4)	0.720(4)	0.748(3)	0.745(3)
Co(3)	*z*	0.246(6)	0.241(5)	0.246(5)	0.248(5)
Co(4)	*z*	0.760(5)	0.756(6)	0.766(5)	0.767(5)
O(1)	*z*	−0.012(6)	−0.003(6)	−0.009(7)	−0.007(6)
O(2)	*z*	0.012(8)	−0.011(8)	0.023(5)	0.022(5)
O(3)	*z*	0.495(8)	0.516(7)	0.485(4)	0.487(5)
O(4)	*x*	−0.006(3)	0.005(2)	−0.016(3)	−0.015(3)
	z	0.311(2)	0.310(2)	0.313(2)	0.312(1)
O(5)	*x*	0.033(2)	0.028(2)	0.012(3)	0.012(3)
	z	0.276(2)	0.275(1)	0.273(1)	0.272(1)
O(6)	*y*	0.227(2)	0.220(2)	0.225(2)	0.225(2)
	z	0.287(3)	0.285(3)	0.307(4)	0.305(4)
O(7)	*y*	0.250(2)	0.257(1)	0.247(2)	0.247(1)
	z	0.700(4)	0.697(3)	0.716(4)	0.714(4)
a (Å)		7.7040(7)	7.7055(6)	7.6579(7)	7.6555(6)
b (Å)		7.8170(7)	7.8179(7)	7.8525(7)	7.8563(7)
c (Å)		7.511(1)	7.5112(9)	7.522(1)	7.5238(9)
R_{wp}		3.83	3.57	3.92	3.59

transitions from the insulating to the metallic state, reflecting the delocalization of charge carriers.[19]

Analysis of the powder patterns collected in the temperature range from 20 to 265 K showed that the magnetic reflections could be indexed on a $2a_p \times 2a_p \times 4a_p$ magnetic unit cell. Various antiferromagnetic models were tested, and it was found that the "antiferromagnetic-phase-3" model for

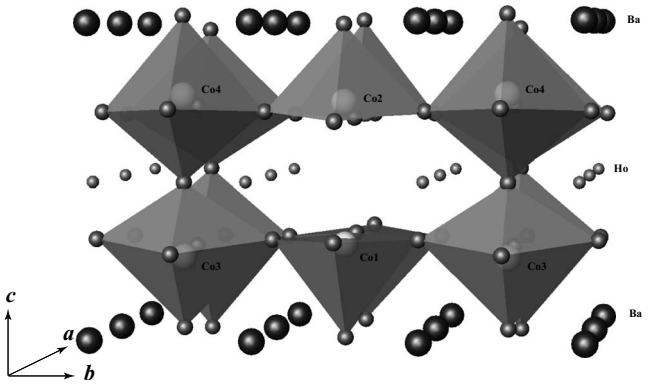

FIG. 2. Structure of $HoBaCo_2O_{5.5}$ at $T=330$ K. Co ions labeled Co(1) and Co(2) are located in pyramidal coordination while Co(3) and Co(4) are coordinated octahedrally.

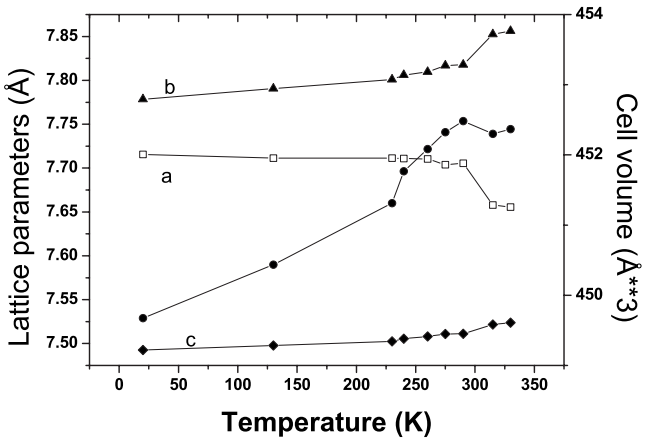

FIG. 3. Lattice parameters and unit cell volume plotted as a function of the temperature. The lines are just guides to the eye. An excess thermal expansion of the volume is observed in the temperature range from 230 to 290 K as explained in the text.

$TbBaCo_2O_{5.5}$ found by Plakhty *et al.*[15] gave a satisfactory description of the measured patterns. This model is derived from a *Pcca* chemical structure by the use of representation theory, and the propagation vector is $\mathbf{k}=0$. The basis vectors for the possible magnetic structures in space group *Pcca* with $\mathbf{k}=0$ have been calculated using the MODY program,[20] and they are listed in the Appendix. The model for magnetic structure of $TbBaCo_2O_{5.5}$ is collinear with magnetic moments parallel to the *x* axis. The model contains formally four independent magnetic moments for the Co ions, but the moments for the Co ions in pyramidal coordination were constrained to have the same value while the moments of the two octahedrally coordinated Co ions were refined independently. The refinements of the chemical and magnetic structure of $HoBaCo_2O_{5.5}$ below 265 K should in principle be done with a *Pcca* model for the chemical structure. However, the limited q range of the present data sets prevents the observation of a possible structural change from space group *Pmma* to *Pcca* as dictated by the magnetic symmetry. The determination of the space group of the magnetically ordered $RBaCo_2O_{5.5}$ compounds is difficult, and it has recently been shown that $DyBaCo_2O_{5.5}$ in contrast to $TbBaCo_2O_{5.5}$ does not transform to a low-temperature phase with *Pcca* symmetry.[21] The *Pmma* space group was therefore retained for the chemical structure of $HoBaCo_2O_{5.5}$ for $T \leqslant 265$ K in the present study. The atomic coordinates were fixed at the values obtained at 275 K, and only lattice parameters and thermal displacement parameters were refined for $T \leqslant 265$ K. This approximation to the chemical structure below 265 K was made to reduce the number of refineable structural parameters. The magnetic unit cell was constructed by doubling of the chemical unit cell along the *c* axis and transforming the Co positions to the doubled unit cell and magnetic moments parallel to the *x* axis were then assigned to the individual Co atoms in the magnetic unit cell in accordance with the model used for $TbBaCo_2O_{5.5}$. Trial refinements showed that the magnetic moments of the Co atoms in pyramidal coordination did not yield reasonable values when refined independently, and they were therefore constrained to have the same magnitude as also was done in the refinements of the magnetic structure of $TbBaCo_2O_{5.5}$.[15] Weighted profile values R_{wp} in the range 3.45–5.17 were obtained in refinements for $T \leqslant 265$ K. Figure 1(b) shows the observed and calculated neutron powder diffraction patterns of $HoBaCo_2O_{5.5}$ at 20 K, and the refined values of the magnetic moments at this temperature as well as the positions of the corresponding Co^{3+} ions in the magnetic unit cell are given in Table II. The magnetic structure at $T=20$ K is shown in Fig. 4. All moments are parallel to the [100] direction, but the structure is rather complex as both ferromagnetic and antiferromagnetic interactions between neighboring Co ions are present in the structure. The coupling along the *a* axis is antiferromagnetic while it is ferromagnetic and antiferromagnetic along the *b* axis for Co ions with $z<\frac{1}{2}$ and $z>\frac{1}{2}$, respectively. The Co ions bridged by the O(3) ions are coupled ferromagnetically along the *c* axis while the remaining couplings along the *c* axis are antiferromagnetic. The spin structure of Co ions in pyramidal and octahedral coordination belongs to the Γ_7 and Γ_8 irreducible representations, respectively. Γ_7 represents ferromagnetic ordering while Γ_8 represents antiferromagnetic ordering. The spins of Co(1) [Py(1) site] and Co(2) [Py(2) site] (both belonging to Γ_7) are coupled antiferromagnetically as is also the case for the Co(3) [Oc(1) site] and Co(4) [Oc(2) site] (both belonging to Γ_8). A ferromagnetic moment will develop along the *x* axis when the magnitudes of the moments on Co(1) and Co(2) are different. This is presumably what is observed near the ordering temperature although refinements of independent moments for the Py(1) and Py(2) sites were unsuccessful with the present sets of data.

TABLE II. Moment values M_N for $HoBaCo_2O_{5.5}$ at 20 K. The magnetic moments M_i are directed along the *x* direction. $M_1=M_2=1.7(1)$, $M_3=3.7(2)$, and $M_4=0.96(9)$ BM at 20 K. Values of the *z* coordinates: $z_{Py(1)}=0.144(2)$ [Co(1)], $z_{Py(2)}=0.365(2)$ [Co(2)], $z_{Oc(1)}=0.123(3)$ [Co(3)], and $z_{Oc(2)}=0.380(3)$ [Co(4)]. The coordinates refer to a $2a_p \times 2a_p \times 2a_p$ magnetic unit cell with lattice parameters $a=7.7163(8)$, $b=7.7791(9)$, and $c=14.983(2)$ Å.

N	*x*, *y*, *z*	M_N
1	$\frac{1}{4}\ 0\ z_{Py(1)}$	M_1
2	$\frac{1}{4}\ 0\ z_{Py(2)}$	$-M_2$
3	$\frac{3}{4}\ 0\ \frac{1}{2}-z_{Py(2)}$	$-M_2$
4	$\frac{3}{4}\ 0\ \frac{1}{2}-z_{Py(1)}$	M_1
5	$\frac{1}{4}\ \frac{1}{2}\ z_{Oc(1)}$	M_3
6	$\frac{1}{4}\ \frac{1}{2}\ z_{Oc(2)}$	$-M_4$
7	$\frac{3}{4}\ \frac{1}{2}\ \frac{1}{2}-z_{Oc(2)}$	$-M_4$
8	$\frac{3}{4}\ \frac{1}{2}\ \frac{1}{2}-z_{Oc(1)}$	M_3
9	$\frac{1}{4}\ 0\ \frac{1}{2}+z_{Py(1)}$	M_1
10	$\frac{1}{4}\ 0\ \frac{1}{2}+z_{Py(2)}$	$-M_2$
11	$\frac{3}{4}\ 0\ -Z_{Py(2)}$	$-M_2$
12	$\frac{3}{4}\ 0\ -z_{Py(1)}$	M_1
13	$\frac{1}{4}\ \frac{1}{2}\ \frac{1}{2}+z_{Oc(1)}$	$-M_3$
14	$\frac{1}{4}\ \frac{1}{2}\ \frac{1}{2}+z_{Oc(2)}$	M_4
15	$\frac{3}{4}\ \frac{1}{2}\ -z_{Oc(2)}$	M_4
16	$\frac{3}{4}\ \frac{1}{2}\ -z_{Oc(1)}$	$-M_3$

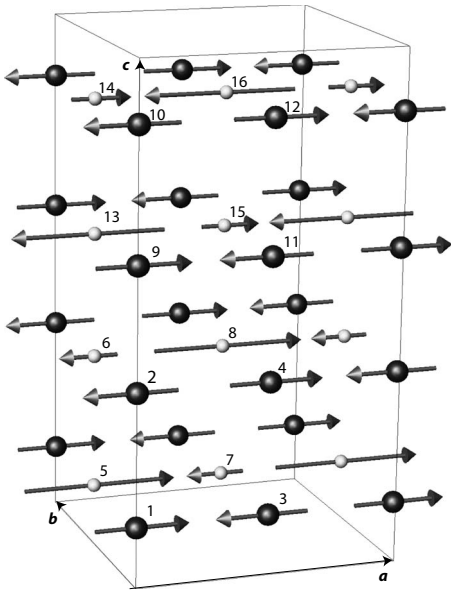

FIG. 4. Magnetic structure of $HoBaCo_2O_{5.5}$ at $T=20$ K. Only Co ions are shown for clarity. Small and large spheres represent Co ions in octahedral and pyramidal coordination, respectively, while the numbers refer to the positions given in Table II. The arrows indicate the magnitude and direction of the magnetic moment on the individual cobalt ions. The shown magnetic unit cell has been translated $\frac{1}{4}$ along the a axis in relation to the coordinates given in Table II for clarity.

The magnitudes of the three different Co magnetic moments are plotted as a function of temperature in Fig. 5. The maximum spin-only values which can be observed by neutron powder diffraction from Co^{3+} ions in the HS and IS states are $4\mu_B$ and $2\mu_B$, respectively. Therefore, the large difference in the magnitude of the observed magnetic moments for the four crystallographically different Co^{3+} ions at low temperature indicates that they are found in different spin states. The observed moments at low temperature shown in Fig. 5 and Table II are in reasonable agreement with the theoretically expected values for the HS states for ions in the Oc(1) site and with the value for the IS states for ions in the Py(1) and Py(2) sites. In contrast, the observed values for the Oc(2) sites are just 48% of the theoretical value for the IS state which makes the assignment of a spin state to the ions in this site difficult. The temperature dependence of the magnetic moment on the Oc(2) site suggests that it is occupied by Co^{3+} ions in the LS ($S=0$) and IS states with the IS state becoming increasingly occupied as the temperature increases.

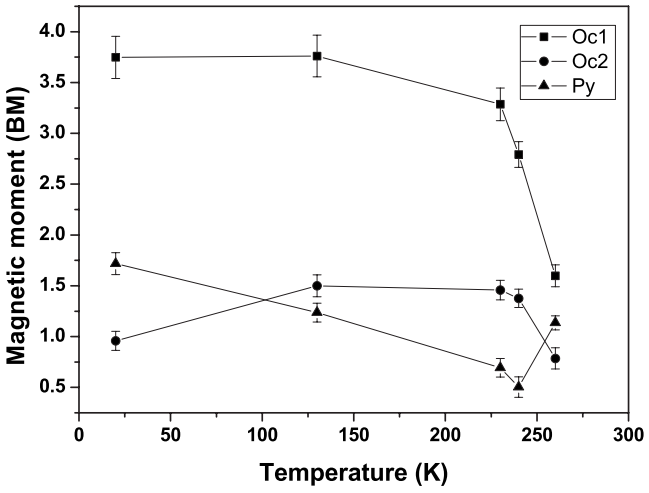

FIG. 5. Magnetic moments for Co^{3+} ions in octahedral and pyramidal sites plotted as a function of temperature. The solid lines are just guides to the eye.

The magnitude of the moment on the Oc(1) site decreases clearly with increasing temperature reflecting an increasing disorder in the magnetic lattice while the magnitudes of the moments on the Oc(2), Py(1), and Py(2) sites show much less pronounced temperature dependence. The fact that the Co ions on the Oc(1) sites are in the HS state is surprising as the crystal field of an octahedral site should be stronger than the corresponding field of a pyramidal site which therefore should favor a lower-spin state of the octahedral site. The assignment of a spin state to a given site is made difficult by the fact that energy differences between different spin states are comparable to thermal energies and excitations from, e.g., the LS to IS state occur at higher temperatures. It is therefore likely that the Oc(2), Py(1), and Py(2) sites contain Co^{3+} ion in both LS to IS states with a ratio changing according to temperature.

The magnetic structure found for $HoBaCo_2O_{5.5}$ in this work is considerably more complex than the magnetic structure of $HoBaCo_2O_5$.[22,23] The magnetic structure of $HoBaCo_2O_5$ was found to be a simple G-type structure in which the Co ions are antiferromagnetically coupled with their six nearest Co neighbors along the three crystallographic axes. The critical temperature for magnetic ordering was found to be 340 K, and a charge-ordering transition during which the Co^{3+} and Co^{2+} ions order along the a axis takes place at 210 K. The Co^{3+} and Co^{2+} ions were both found to be in the HS state, and the G-type magnetic structure of $HoBaCo_2O_5$ is fully supported by the Goodenough-Kanamori (GK) rules for superexchange magnetism.[24,25] The complex magnetic structure of $HoBaCo_2O_{5.5}$ contains both positive and negative exchange interactions between nearest neighbors. The signs of the superexchange interactions and thereby the magnetic structure are hardly predictable by using the GK rules and reasonable assumptions about orbital occupancies. Recently, the magnetic structure of $YBaCo_2O_{5.5}$ has been studied by Khalyavin *et al.*[26] The crystal structure was refined in space group *Pmma* for $T>190$ K, and a spin-state-ordered magnetic phase was observed in the temperature range from 190 to 265 K. The magnetic phase contains octahedrally coordinated Co^{3+} ions in the LS and HS states, forming chessboardlike spin-state-ordered (ac) planes, while the pyramidally coordinated Co^{3+} ions adopt the HS state. The magnetic structure of $YBaCo_2O_{5.5}$ observed in the temperature range from 190 to 265 K has several similarities in common with the magnetic structure of $HoBaCo_2O_{5.5}$ observed in this study as well as with the "antiferromagnetic-phase-3" model for $TbBaCo_2O_{5.5}$.[15] However, the Co^{3+} ions located in the Oc(2) sites were not found to be in the LS state as observed in the case of $YBaCo_2O_{5.5}$. The observed mag-

netic moments on the Oc(2) site might be induced by a small degree of imperfect oxygen ordering in the $[HoO_{0.5}]$ layer, which gives raise to misplaced pyramids, as suggested by Frontera *et al.* in their study of $PrBaCo_2O_{5.5}$.[27]

IV. CONCLUSION

The chemical structure of $HoBaCo_2O_{5.5}$ in the paramagnetic phase above 265 K has been refined in space group *Pmma* using a $2a_p \times 2a_p \times 2a_p$ unit cell. It was found that the *a* and *b* axes decrease and increase abruptly between 290 and 315 K which presumably is due to the melting of orbital order which accompanies the MI transition. Furthermore, an excess thermal expansion was observed in the temperature range from 230 to 290 K followed by a minor drop in the unit cell volume between 290 and 315 K. The excess volume expansion is most likely due to a change in spin state of the Co ions while the drop in the unit-cell volume is due to delocalization of electrons associated with the transition from the insulating to the metallic state. In contrast to $TbBaCo_2O_{5.5}$, which undergoes a *Pmmm* to *Pmma* transition at the magnetic transition,[15] no indication of structural phase transitions was found within the investigated temperature range. The magnetic structure of $HoBaCo_2O_{5.5}$ was shown to be antiferromagnetic with a $2a_p \times 2a_p \times 4a_p$ magnetic unit cell containing four crystallographically independent Co ions. The structure is relatively complex as it contains both ferromagnetic and antiferromagnetic interactions. The Co ions in octahedral Oc(1) sites were found to be in the HS state while the Co ion in the octahedral Oc(2) sites was found to be in a mixed LS and IS state. The Co ions in the two crystallographically different pyramidally sites were constrained to have the same magnetic moment, and the refined low temperature value of this moment indicates that these ions are in the IS state.

ACKNOWLEDGMENTS

This work was performed at Swiss Spallation Source, Paul Scherrer Institute, Villigen, Switzerland, and the authors are grateful to the machine and beamline groups whose outstanding efforts have made the experiment possible. DANSCATT is acknowledged for financial support.

APPENDIX

The basis functions of the irreducible group representations (IR) for the $4d$ $(1/4\ 0\ z)$ and $4e$ $(1/4\ 1/2\ z)$ positions in space group *Pcca* with $\mathbf{k}=0$ were calculated using the MODY program.[20] Eight one-dimensional irreducible representations Γ_i enter the reducible (12×12)-dimensional magnetic representation:

$$\Gamma = \Gamma_1 + \Gamma_2 + 2\Gamma_3 + 2\Gamma_4 + \Gamma_5 + \Gamma_6 + 2\Gamma_7 + 2\Gamma_8,$$

$4d(\frac{1}{4}\ 0\ z)$ position,

	Γ_1	Γ_2	Γ_3		Γ_4		Γ_5	Γ_6	Γ_7		Γ_8	
$\frac{1}{4}\ 0\ z$	0	0	0	1	0	1	0	0	0	1	0	1
	0	0	1	0	1	0	0	0	1	0	1	0
	1	1	0	0	0	0	1	1	0	0	0	0
$\frac{3}{4}\ 0\ \frac{1}{2}-z$	0	0	0	−1	0	−1	0	0	0	1	0	1
	0	0	1	0	1	0	0	0	−1	0	−1	0
	−1	−1	0	0	0	0	1	1	0	0	0	0
$\frac{3}{4}\ 0\ -z$	0	0	0	1	0	−1	0	0	0	1	0	−1
	0	0	1	0	−1	0	0	0	1	0	−1	0
	1	−1	0	0	0	0	1	−1	0	0	0	0
$\frac{1}{4}\ 0\ \frac{1}{2}+z$	0	0	0	−1	0	1	0	0	0	1	0	−1
	0	0	1	0	−1	0	0	0	−1	0	1	0
	−1	1	0	0	0	0	1	−1	0	0	0	0

$4e(\frac{1}{4}\frac{1}{2}\ z)$ position,

	Γ_1	Γ_2	Γ_3		Γ_4		Γ_5	Γ_6	Γ_7		Γ_8	
$\frac{1}{4}\ \frac{1}{2}\ z$	0	0	0	1	0	1	0	0	0	1	0	1
	0	0	1	0	1	0	0	0	1	0	1	0
	1	1	0	0	0	0	1	1	0	0	0	0
$\frac{1}{4}\ \frac{1}{2}\ \frac{1}{2}-z$	0	0	0	−1	0	−1	0	0	0	−1	0	1
	0	0	1	0	1	0	0	0	1	0	−1	0
	−1	−1	0	0	0	0	1	1	0	0	0	0
$\frac{3}{4}\ \frac{1}{2}\ -z$	0	0	0	1	0	−1	0	0	0	1	0	−1
	0	0	1	0	−1	0	0	0	1	0	−1	0
	1	−1	0	0	0	0	1	−1	0	0	0	0
$\frac{1}{4}\ \frac{1}{2}\ \frac{1}{2}+z$	0	0	0	−1	0	1	0	0	0	1	0	−1
	0	0	1	0	−1	0	0	0	−1	0	1	0
	−1	1	0	0	0	0	1	−1	0	0	0	0

*Corresponding author.

[1] A. Maignan, C. Martin, D. Pelloquin, N. Nguyen, and B. Raveau, J. Solid State Chem. **142**, 247 (1999).
[2] Y. Moritomo, M. Takeo, X. J. Liu, T. Akimoto, and A. Nakamura, Phys. Rev. B **58**, R13334 (1998).
[3] W. Zhou, C. Tian Lin, and W. Yao Liang, Adv. Mater. (Weinheim, Ger.) **5**, 735 (1993).
[4] T. Vogt, P. M. Woodward, P. Karen, B. A. Hunter, P. Henning, and A. R. Moodenbaugh, Phys. Rev. Lett. **84**, 2969 (2000).
[5] J. C. Burley, J. F. Mitchell, S. Short, D. Miller, and Y. Tang, J.

Solid State Chem. **170**, 339 (2003).
[6] S. Sugano, Y. Tanabe, and H. Kamimura, *Multiplets of Transition-Metal Ions in Crystals* (Academic Press, New York 1970).
[7] M. A. Korotin, S. Yu. Ezhov, I. V. Solovyev, V. I. Anisimov, D. I. Khomskii, and G. A. Sawatzky, Phys. Rev. B **54**, 5309 (1996).
[8] M. Imada, A. Fujimori, and Y. Tokura, Rev. Mod. Phys. **70**, 1039 (1998).
[9] D. D. Khalyavin, I. O. Troyanchuk, N. V. Kasper, Q. Huang, J. W. Linn, and Szymczak, J. Mater. Res. **17**, 838 (2002).
[10] F. Fauth, E. Suard, V. Caignaert, and I. Mirebeau, Phys. Rev. B **66**, 184421 (2002).
[11] M. Soda, Y. Yuasui, T. Fujita, T. Miyashita, M. Sata, and K. Kakura, J. Phys. Soc. Jpn. **72**, 1729 (2003).
[12] A. A. Taskin, A. N. Lavrov, and Y. Ando, Phys. Rev. Lett. **90**, 227201 (2003).
[13] M. Soda, Y. Yuasui, M. Ito, S. Iikubo, M. Sata, and K. Kakura, J. Phys. Soc. Jpn. **73**, 2857 (2004).
[14] Y. Morimoto, T. Akimoto, M. Takeo, A. Machida, E. Nashibori, M. Takata, M. Sakata, K. Ohoyama, and A. Nakamura, Phys. Rev. B **61**, R13325 (2000).
[15] V. P. Plakhty, Yu. P. Chernenkov, S. N. Barilo, A. Podlesnyak, E. Pomjakushina, E. V. Moskvin, and S. V. Gavrilov, Phys. Rev. B **71**, 214407 (2005).
[16] J. Rodríguez-Carvajal, Physica B **192**, 55 (1993).
[17] C. Frontera, J. L. García-Muñoz, A. Llobet, M. A. G. Aranda, J. Rodriguez-Carvajal, M. Respaud, J. M. Broto, B. Raquet, H. Rakoto, and M. Goiran, J. Alloys Compd. **323-324**, 468 (2001).
[18] C. Frontera, J. L. García-Muñoz, A. Llobet, and M. A. G. Aranda, Phys. Rev. B **65**, 180405(R) (2002).
[19] E. Pomjakushina, K. Conder, and V. Pomjakushin, Phys. Rev. B **73**, 113105 (2006).
[20] W. Sikora, F. Białas, and L. Pytlik, J. Appl. Crystallogr. **37**, 1015 (2004).
[21] Yu. P. Chernenkov, V. P. Plakhty, A. G. Gukasov, S. N. Barilo, S. V. Shiryaev, G. L. Bychkov, V. Hinkov, V. I. Fedorov, and V. A. Chekanov, Phys. Lett. A **365**, 166 (2007).
[22] F. Fauth, E. Suard, V. Caignaert, B. Domengès, I. Mirebeau, and L. Keller, Eur. Phys. J. B **21**, 163 (2001).
[23] E. Suard, F. Fauth, V. Caignaert, I. Mirebeau, and G. Baldinozzi, Phys. Rev. B **61**, R11871 (2000).
[24] J. B. Goodenough, Phys. Rev. **100**, 564 (1955).
[25] J. Kanamori, J. Phys. Chem. Solids **10**, 87 (1959).
[26] D. D. Khalyavin, D. N. Argyriou, U. Amann, A. A. Yaremchenko, and V. V. Kharton, Phys. Rev. B **75**, 134407 (2007).
[27] C. Frontera, J. L. Garcia-Munoz, A. E. Carrillo, M. A. G. Aranda, I. Margiolaki, and A. Caneiro, Phys. Rev. B **74**, 054406 (2006).